Pre-trained Bi-LSTM model for automated classification of ventricular arrhythmias using 1-D and 2-D ECG

M Krishna Chaitanya, Lakhan Dev Sharma
School of Electronics Engineering, VIT-AP University, Amaravati, India

Article Info

ABSTRACT

Number of cardiac conditions have been associated with abnormal heartbeat (arrhythmia) such as ventricular fibrillation (Vfib), ventricular flutter (Vfl), and ventricular tachycardia (Vta). This is a difficult and essential job for timely clinical assessment and identification of these potentially life-threatening heart arrhythmias. With the aid of a one-dimensional electrocardiogram (ECG) signal and its associated two-dimensional image, the suggested method provides a strategy for the detection of time-frequency interpretation (Vfib, Vfl, and Vta). A four-stage cascaded Savitzky-Golay (SG) filter is used after a 2-stage median filter to preprocess the ECG signal. This technique employs z-score normalisation after brief (2 sec) ECG readings. The classification of these ECG segments (1-D) and associated time-frequency representation pictures (2-D) was explored separately using a bi-directional long short-term memory-based network. Eight distinct categorization scenarios were examined, and then an average accuracy of 99.67% for 1-D ECG and 99.87% for 2-D ECG signal was attained.

Corresponding Author:

Lakhan Dev Sharma
School of Electronics Engineering, VIT-AP University
Amaravati, 522237, India
Email: devsharmalakhan@gmail.com

1. INTRODUCTION

The physiological functions of the heart are electrically portrayed by the electrocardiogram (ECG) [1]. Any alteration in the ECG signal's morphology indicates a heart problem. Cardiovascular diseases are the major cause of death worldwide, and not just in middle- and lower-income nations [2], [3]. The most frequent reasons for cardiovascular fatalities are ventricular fibrillation (Vfib), ventricular flutter (Vfl), and ventricular tachycardia (Vta) [4]. In order to effectively treat Vfib and Vta patients, automatic external defibrillators (AEDs) as well as implanted cardioverter defibrillators (ICDs) should be able to distinguish between Vfib and Vta successfully and consistently [5]. Therefore, accurate and prompt detection of cardiac problems may contribute to preventing mortality from heart failure or stroke [6]. Manual ECG analysis requires a high level of expertise from the cardiologist in order to detect cardiovascular problems. The ECG is normally examined by a cardiologist to look for irregularities, which renders the process lengthy and frustrating and reduces the diagnostic effectiveness [7]. Three distinct classes of premature ventricular contractions (PVC, normal, and all other beats as one class) are identified in [8]. The application of statistics to the features that characterise ECG signals was demonstrated in [9]. The development of multilayer perceptron (MLP) neural network designs that can recognise ECG signal variability is described in [9]. They have proposed a three-stage method made up of units for denoising, feature extraction, and classification. Despite the fact that there were very few recordings

collected for the experiment, the precision was not as intended. The ECG signal is preprocessed by employing discrete wavelet transform, extracted the statistical features and are fed to the support vector machine (SVM) for categorization [10]. Castro *et al.* [11] extracted the characteristics like heart rate variability, pressure wave (P-Wave), and QRS complex from the ECG and fed to feedforward neural network for categorization of paroxysmal atrial fibrillation. Nugroho *et al.* [12] proposed an efficient model which can able to forecast coronary artery diseases and acheived good accuracy by effectively tuning hyperparametrs.

Recently, especially with the application of artificial intelligence (AI), automatic categorization of different cardiac problems has increased tremendously. Asmae *et al.* [13], a synthetic minority oversampling strategy is used to address issues with imbalanced classes. To conduct an empirical assessment, many researchers employed long short-term memory (LSTM), bidirectional long short-term memory (Bi-LSTM) [14]–[19]. Using an unbalanced dataset, atrial fibrillation (Afib) was automatically classified in [20] using a hybrid convolutional neural network (CNN)-LSTM approach. As it can be applied directly to one dimensional recurrent neural network (RNN) as well as CNN models, deep learning (DL) may be utilised to achieve one-dimensional ECG data classification. Consequently, using an AI model designed for a 2-D image to characterize a 1-D signal is not possible [7]. As a result, processing the 1-D ECG signal for arrhythmia classification using 2-D image classification approaches is best accomplished through signal conversion into the spectral domain. Time-frequency approximations have been employed in many applications for efficient interpretation of non-stationary signals like sonar, radar, biological, multimedia data, seismic, and more. Utilizing temporal frequency distributions is the most widely used technique [21]. For a variety of frequency-modulated signals, several scientists have diligently attempted to identify an ideal distribution [22]–[24] There have been several time-frequency distributions proposed.

After segmentation and preprocessing, our proposed approach prepares the dataset by utilising z-score normalisation. The one-dimensional ECG data was transformed into the model's two-dimensional visual representation in order to use it (i.e., in time-frequency domain). Our suggested solution makes use of a Bi-LSTM oriented DL model to classify ECG in both 1-D and 2-D. The paper is formatted as follows: the databases used for this study and underlying methodology for this suggested technique are discussed in section 2. The findings are presented in section 3, the discussion is presented in section 4, and a succinct conclusion is presented in section 5.

2. MATERIALS AND METHOD

The ECG datasets used in this study were taken from the MIT-BIH malignant ventricular ectopy database (MVED) and creighton university ventricular tachyarrhythmia database (CUVDB) [25], [26]. 35 eight-minute ECG recordings of human patients with sustained spells of Vta, Vfl, or Vfib can be found in the CUVDB. The MVED has 22 half-hour ECG recordings of individuals who experienced persistent ventricular tachycardia, ventricular fibrillation, and ventricular flutter. From each record, required slices are selected depending on the annotations. CUVDB contains 35 eight-minute ECG recordings of human subjects who had sustained Vfib, Vfl, and Vta episodes. These rhythms are incredibly difficult to capture in high-quality, making them crucial for the creation and assessment of ventricular arrhythmias [25].

In this section, we provide our proposed method for automatic Vfl, Vfib, and Vta categorization using an ECG image AI-based idea. The five steps of the methodology include preprocessing, segmentation, 2-D image conversion, normalisation, and Bi-LSTM. Figure 1 shows the proposed technique's process flow.
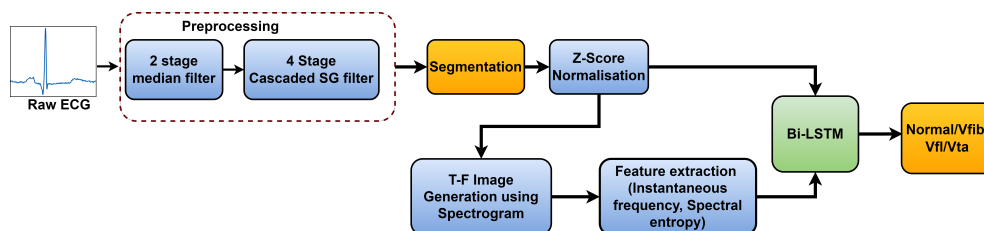

Figure 1. Work flow of the proposed technique

2.1. Pre processing

The dominant noises in the raw ECG signal are baseline line wander (BW) as well as powerline interference (PLI). The technique's performance is considerably improved by reducing contamination from the original ECG, which is an essential phase. The noise present in the signal makes it difficult to identify the state of the heart. To obtain a BW free ECG at the preprocessing stage, the raw ECG signal is passed via a two-stage median filter [27]. The PLI noise contained in the ECG signal is then removed using a four-stage Savitzky-Golay (SG) filter [28].

2.2. Segmentation and normalisation

Both datasets contain lengthy ECG records that need to be split before being fed into a DL algorithm. After preprocessing for investigation, long-term ECG signals are divided into short-term ECG segments (2 sec). 500 samples, which are enough for the DL model, are present in a 2-second slice [29], [30]. Figures 2(a) to (d) show the segments of the normal, Vfib, Vfl, and Vta signals, respectively.
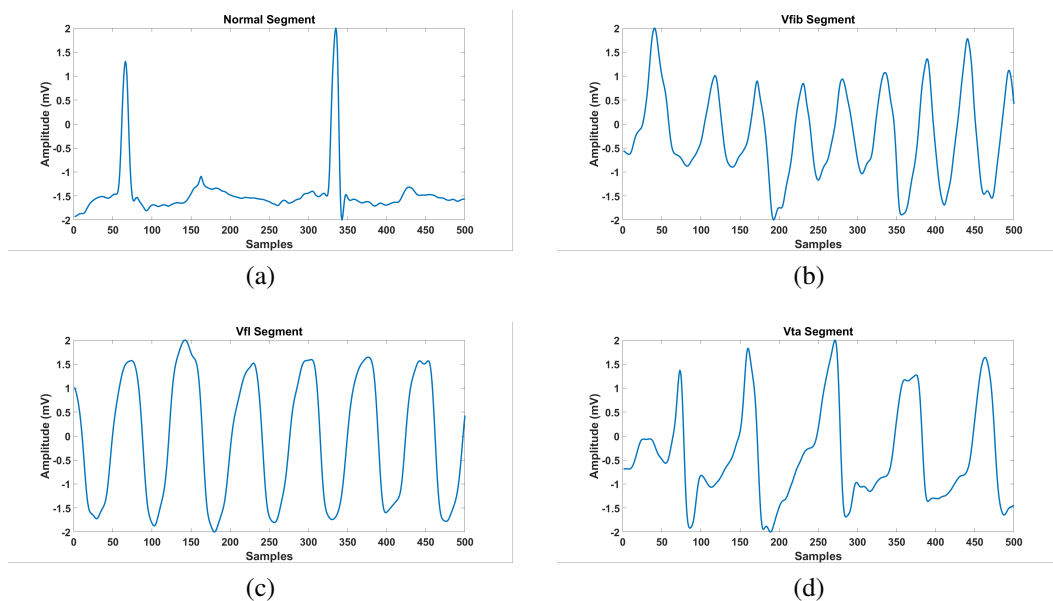

Figure 2. Sample segments of; (a) normal heartbeat rhythm segment, (b) ventricular fibrillation segment, (c) ventricular flutter segment, and (d) ventricular tachycardia segment

The segmented ECG signal is then normalised. By maintaining the signal inside the range, this method enables DL models to train more rapidly and accurately. To normalise the signal, the z-score method was employed. The mathematical formula is provided by (1):

$$x(n) = \frac{h(n) - \mu}{\sigma} \tag{1}$$

where $h(n)$ denotes original signal, $x(n)$ represents the normalised signal, μ is mean, and σ is standard deviation.

2.3. Time-frequency image conversion

The time-frequency (T-F) image is a 2-D (2-D) representation of the energy distribution of a signal. The frequency content of a signal is described by prior spectrum analysis techniques without revealing the precise locations of the signal's individual frequency components. The short-term Fourier transform is used to receive the frequencies in each sector of the spectrogram, which divides the signal into shorter terms (STFTM). By a spectrogram of smaller sections, the normalised and square magnitude of the STFTM parameters are displayed. The energy present in the STFTM spectrogram [31] is equal to the energy in the time–frequency signal. Figures 3(a) to (d) depicts time-frequency representations of normal, Vfib, Vfl, and Vta segments respectively.
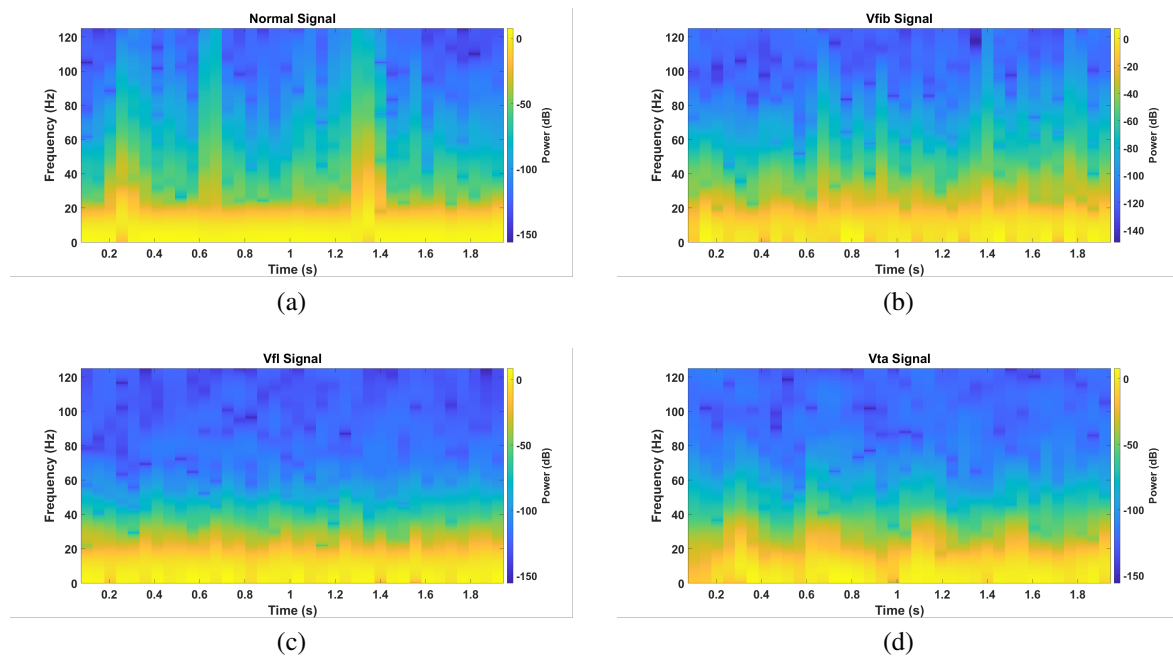
Figure 3. 2-D representation of; (a) normal, (b) Vfib, (c) Vfl, and (d) Vta signals

2.4. Feature extraction

The effectiveness of the proposed method can be improved by feature extraction, such as instantaneous frequency ($f_{ins}(t)$) and spectrum entropy (SPEN). The signal time-dependent frequency, which was obtained using (2), is determined by the $f_{ins}(t)$ [32].

$$f_{ins}(t) = \frac{\int_0^\infty f Q(t,f) df}{\int_0^\infty Q(t,f) df} \tag{2}$$

where $Q(t,f)$ is spectrogram power spectrum of the ECG signal.

The distribution of the signal spectrum is also computed by SPEN using the distribution power spectrogram. The normalised power distribution's Shannon entropy is computed in the frequency domain by the SPEN, which interprets the signal as a probability distribution. A signal's power spectrum as well as probability distribution function is used to generate the SPEN equation. In (3) Vakkuri *et al.* [33] was used to compute the SPEN:

$$SPEN = -\sum_{m=1}^{N} Q(m) \log_2 Q(m) \tag{3}$$

where $Q(m)$ is the probability distribution.

2.5. Bidirectional long short term memory

The LSTM was developed by Hochreiter and Schmidhuber to overcome vanishing gradient problems, particularly in ANN designs [34]. A kind of RNN called LSTM is used to handle sequential data processing, including voice identification, genome exploration, image categorization, as well as other classifications [35]. The ANN's inability to handle temporal data well and its dependency on previous input for future input are two issues that the RNN network resolves. A hidden layer resembling memory cells is used by LSTM [36]. The three gates: the input gate (i_g), output gate (o_g), and forget gate (f_g), govern the memory unit, which saves the temporal information traveling through it. The i_g checks the input sequence and prior concealed state to see if the input is still worth saving, and then utilises it to gate new memory module. The f_g is identical to the i_g, but it does not use the input sequence to determine whether or not the preceding memory unit may be used to estimate the current memory unit. In the LSTM, the o_g is not clearly visible. These gates provide

ranges between zero and one by using the sigmoid as an activation function. A value of 0 in the activation function denotes a closed gate, while a value of 1 denotes an open gate. No data can pass through the gate when it is closed, but all data can pass through when the gate is released [37]. The internal structure of a single LSTM unit is shown in Figure 4. The LSTM cell's restrictions, which only permit the use of previous data, must be circumvented. Schuster and Paliwal [38] proposed bidirectional recurrent neural networks (BiRNNs), that are composed of two separate LSTM hidden layers with similar output but in opposite directions. This design uses insights from the past and the future in the output layer. In Bi-LSTM, an input sequence X = (X1, X2, ..., Xn) is calculated in the forward direction as $\overrightarrow{h_f} = (\overrightarrow{h_1}, \overrightarrow{h_2}, \overrightarrow{h_3}......\overrightarrow{h_n})$ and backward directions as $\overleftarrow{h_b} = (\overleftarrow{h_1}, \overleftarrow{h_2}, \overleftarrow{h_3}....\overleftarrow{h_n})$. This cell's final out is created by both h_f and h_b the final sequence of out reads y = (y1, y2, y3 ..., yn). The basic structure of Bi-LSTM network is depicted in the Figure 5.
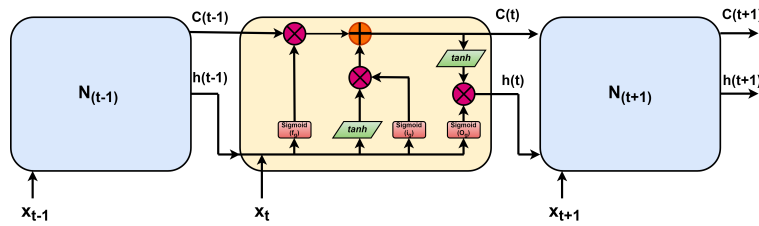

Figure 4. Architecture of an LSTM unit

The Bi-LSTM network is designed with a sequence input layer, where the sequence input is equal to one for a 1-D representation and two for a 2-D representation. Next comes a 100-hidden-unit Bi-LSTM layer, then a fully connected layer with a 4-dimensional inner space, and finally an activation function titled softmax in the output layer. The "crossentropyex" loss function-based final classification layer follows the fully connected layer. In (4)-(8) describe the mathematical specifics for the gates in Bi-LSTM:

$$f_g = sigmoid(W_{xf}x_t + W_{fh}h_{t-1}) + b_f \tag{4}$$

$$i_g = sigmoid(W_{ix}xt + W_{ih}h_{t-1} + b_i) \tag{5}$$

$$o_g = sigmoid(W_{ox}x_t + W_{oh}h_{t-1} + b_o) \tag{6}$$

$$c_t = c_{t-1} \odot f_g + i_g \odot tanh(W_{cx}x_t + W_{ch}h_{t-1} + b_c) \tag{7}$$

$$h_t = o_g \odot tanh(c_t) \tag{8}$$

where c_t denotes current state cell, h_t represents current hidden state, and $\odot$ depicts element-wise multiplication of vectors.
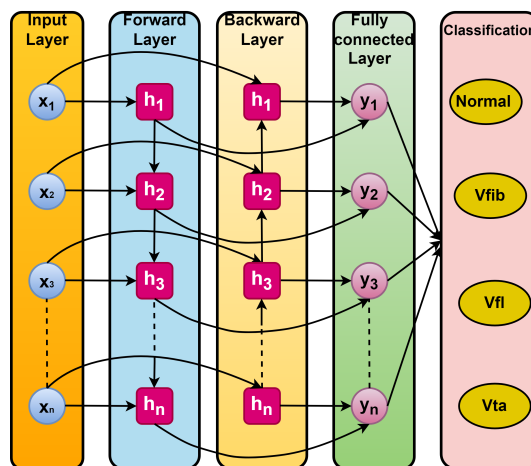

Figure 5. Basic organization of Bi-LSTM network

3. RESULTS

Data from CUVDB and MVED were used to evaluate the method's performance for four distinct categories of Vfib, Vfl, Vta, as well as normal. MATLAB 2020a software was used to conduct the experiments on a desktop computer with an Intel i7-series processor running at 3.12 GHz and 16 GB of RAM. In this work, the identification of normal, Vfib, Vfl, as well as Vta in 1-D and 2-D representations was carried out using the Bi-LSTM, and the outcomes were verified using other established methods. The 10-fold cross-validation process of the LSTM model was used to train and evaluate the proposed neural network model. For the Bi-LSTM model to perform classification during research, the following aspects were chosen: Adam was chosen as the optimizer, with a batch size of 100 and a learning rate of 0.01. Each investigation was simulated with the 30 epochs in consideration to ensure the consistency of the model. For binary class classification, a total of 11396 normal, 1200 Vfib, 1000 Vfl, and 1200 Vta segments are utilised. 90 percent of them i.e., 10360, 1080, 900, and 1080 samples of normal, Vfib, Vfl, and Vta, respectively, were used for training and the rest 10 percent of the data i.e., 1036 normal, 120 Vfib, 100 Vfl, and 120 Vta is employed for testing.

The results are presented on binary class classification utilizing two approaches: 1-dimensional ECG and its time–frequency representation as inputs. Table 1 depicts the confusion matrix (CMX) elements obtained by using test data for different classification strategies. To assess the classification's performance, we employed performance metrics such as accuracy (ACCY%), sensitivity (SEN%), specificity (SPY%), and positive pre-dictivity (PP%). The metrics mentioned afore were calculated using:

$$ACCY\% = \frac{(TP + TN)}{(TP + TN + FN + FP)} \times 100 \qquad (9)$$

$$SEN\% = \frac{(TP)}{(TP + FN)} \times 100 \qquad (10)$$

$$SPY\% = \frac{(TN)}{(TN + FP)} \times 100 \qquad (11)$$

$$PP\% = \frac{(TP)}{(TP + FP)} \times 100 \qquad (12)$$

where TP denotes true positive, FP represents false positive, TN is true negative, and FN denotes false negative.

Table 1. CMX and performance metrics calculations

Input	Experimentation	TP	FP	FN	TN	SEN(%)	SPY(%)	PP(%)	ACCY(%)
1-D	Normal Vs Vfl	100	0	4	1032	96.15	100	100	99.65
	Normal Vs Vfib	120	0	1	1035	99.17	100	100	99.91
	Vfib Vs Vfl	100	0	0	120	100	100	100	100
	Normal Vs Vta	119	1	4	1032	96.75	99.9	99.17	99.57
	Vfib Vs Vta	120	0	1	119	99.17	100	100	99.58
	Vfl Vs Vta	100	0	1	119	99.01	100	100	99.55
	Normal Vs Vfib + Vfl	213	7	3	1033	98.61	99.33	96.82	99.2
	Normal + Vfl Vs Vfib	120	0	1	1135	99.17	100	100	99.92
	Average	124	1	1.88	703.13	98.50	99.90	99.50	99.67
2-D	Normal Vs Vfl	100	0	3	1033	97.09	100	100	99.74
	Normal Vs Vfib	119	1	2	1034	98.35	99.9	99.17	99.74
	Vfib Vs Vfl	100	0	0	120	100	100	100	100
	Normal Vs Vta	119	1	1	1135	99.17	99.91	99.17	99.84
	Vfib Vs Vta	120	0	0	120	100	100	100	100
	Vfl Vs Vta	100	0	0	120	100	100	100	100
	Normal Vs Vfib + Vfl	219	1	4	1032	98.21	99.9	99.55	99.6
	Normal + Vfl Vs Vfib	120	0	0	1036	100	100	100	100
	Average	124.63	0.38	1.25	703.75	99.10	99.96	99.74	99.87

3.1. Experimentation with 1-D electrocardiogram

When no additional features could be recovered in this experiment, the output from the Bi-LSTM prototype using 1-D ECG was obtained. After preprocessing, segmentation, and normalisation, the database was subsequently compelled to use Bi-LSTM for classification. This dataset was divided into segments that

were each 1×500 pixels long. The Bi-LSTM prototype used in this study uses a bi-directional LSTM layer (100 hidden units), a fully linked layer (4 units, softmax activation), and a final output classification layer to produce the results (crossentropyex loss function).

The experimental results obtained using 1-D ECG are depicted in the Table 1 under the row labeled '1-D'. From the Table 1 under the row labeled '1-D', we infer that we have achieved ACCY% of 100 in the case of Vfib Vs. Vfl. The average ACCY% obtained for different classification strategies is 99.67. The average SEN%, SPY%, and PP% obtained for different classification strategies are 98.5, 99.9, and 99.5 respectively.

3.2. Experimentation using time–frequency (2-D) representation of electrocardiogram

In this study, the dataset for the Bi-LSTM structure was created using the 2-D ECG format. The 1-D ECG data's time-frequency description was produced via the spectrogram. The instantaneous frequency and spectral entropy of the spectrum were computed for each segment of the dataset. The time-frequency representation of the ECG was combined with the Bi-LSTM model for categorization. The developed model is put to the test using several categorization strategies, which are discussed in the preceding section.

The experimental results obtained using 2-D ECG are depicted in the Table 1 under the row labeled '2-D'. From the Table 1 under the row labeled '2-D', we infer that we have achieved highest ACCY% of 100 in the case of Vfib Vs Vfl, Vfib Vs Vta, and Vfl Vs Vta. The average ACCY% obtained for different classification strategies is 99.87. The average SEN%, SPY%, and PP% obtained for different classification strategies are 99.1, 99.96, and 99.74 respectively. We have also performed the experimentation for different epoches. The plot showing various accuracies against different epoches for different cases of 1-D and 2-D ECGs is shown in the Figure 6(a) and Figure 6(b) respectively.
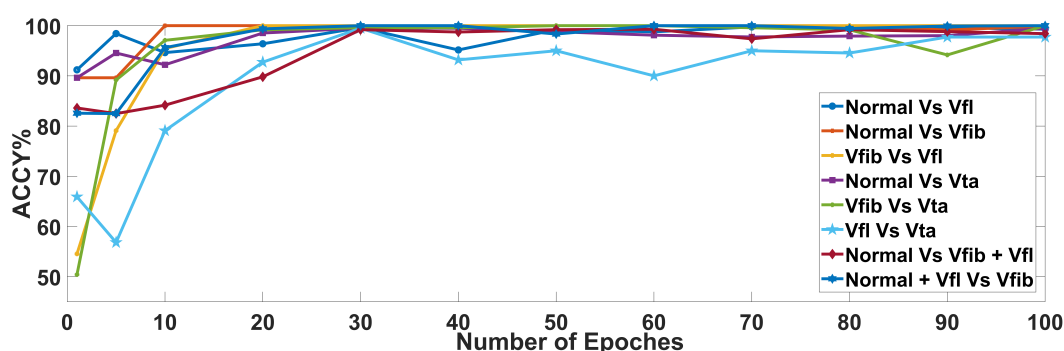
(a)
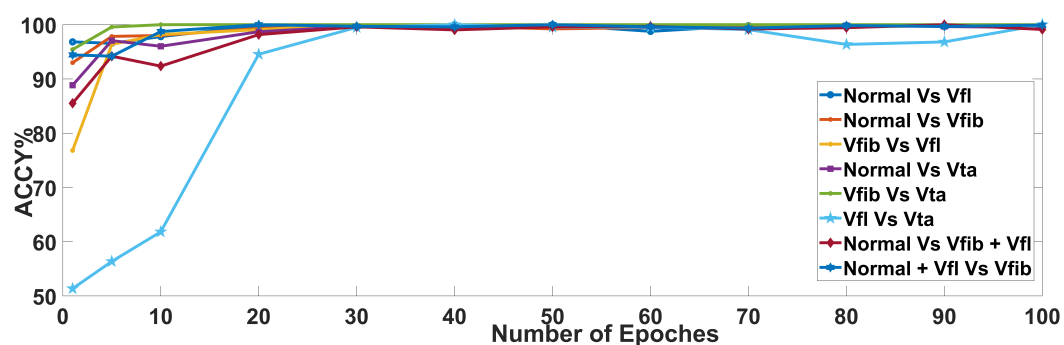
(b)

Figure 6. Plot showing the number of epoches against ACCY% for different cases of; (a) 1-D and (b) 2-D ECG

4. DISCUSSION

In prior investigations, the feature extraction stage was used to create data for the feeding classifier that was used to identify Vfib, Vfl, and Vta. As far as we are aware, that also happens with every arrhythmia

detection method and every categorization technique that relies on biological data [39]. No matter whether a signal's components are from the frequency domain, the time domain, or the cardiac cycle, features are thought to collect information that is relevant to class discrimination [40]. Thus, deciding which attributes should have been used as classifier input has turned into an usual challenge for learning algorithms [39]. First, we hypothesised that since features are presumed either explicitly or implicitly from 1-D or 2-D anatomical structure of the ECG signal, time-frequency depiction images could be directly fed into any classification model to achieve the best results, provided that time and frequency details are preserved without any loss [41]. We concentrated on recognising and differentiating normal, Vfib, Vfl, and Vta despite keeping the extent of preprocessing necessary to a minimum in order to verify our hypotheses. The proposed method is contrasted with a number of other methods in Table 2.

Table 2. Comparison of the proposed technique with various existing methods

Author	Method	Input	Type of arrhythmias	Performance metrics		
				ACCY(%)	SEN(%)	SPY(%)
Current	Bi-LSTM with Z-score NRSN	1-D	Nl, Vfib, Vfl, and Vta	99.67	98.5	99.9
		2-D	Nl, Vfib, Vfl, and Vta	99.87	99.1	99.96
[42]	SVM + AdaBoost	1-D	Vfib	98.20	98.25	98.18
[30]	CNN	1-D	Vfl Vs Vta Scenario	81.25	90.46	70.82
[43]	2-D CNN	2-D	Shockable rhythms	98.82	95.05	99.43
[41]	ANN	2-D	Vfib,Vta	98.19	95.56	98.8
	BGC	2-D	Vfib,Vta	98.44	98.46	98.43
[44]	DAS	1-D	Vfib		94.1	93.8
[45]	SVM	1-D	Vfib	96.3	96.2	96.3
[5]	AEY	1-D	Vfib	91	91.84	90.2
[4]	KNNS	1-D	Vfib	93.2	98.1	88
[4]	RNFN	1-D	Vfib	91.3	91.53	90.91
	RFAM			95.66	95.37	95.96
	SVM	1-D	Vfib Vta Vs Non-Vfib Vta scenario	89.58	82.02	97.08
[46]	KNN			96.01	95.64	96.38
	RFAM			95.8	95.74	95.86
	SVM	1-D	Vfib Vs non-Vifb scenario	89.3	81.84	96.86
	KNN			93.22	93.73	95.31
[47]	RFAM	1-D	Vfib	91.3	91.84	90.2
[5]	FSAE	1-D	Vfib	97.5	97.98	97.03
[48]	EMDAE	1-D	Vfib	91.2	90.47	91.66

Nl: normal, Afibn: atrial fibrillation, Aflr: atrial flutter, RQAS: recurrence quantification analysis, RNFN: radial basis function, EM-DAE: emperical mode decomposition and app entropy, FSAE: fuzzy simil app entropy, KNNS: K-nearest neighbors, DWTPCA: discrete wavelet transform with principal component analysis, DB6C: daubechies-6 with counters, BGC: bagging classifier, DAS: discriminant analysis, AEY: approximate entropy, NRSN: normalisation.

Approximate entropy is used for distinguishing between Vfib and Vta and achieved a good performance, i.e, ACCY% of 91, SEN% of 91.8, and SPY% of 90.2 [5]. SVM is used and was able to achieve an ACCY%=96.3, SEN%=96.2, and SPY%=96.2% [45]. Amalgamation of SVM and AdaBoost and achieved ACCY% of 98.20, 98.25 SENY%, and 98.18 SPY% [42]. Panda *et al.* [30] utilizes deep CNN and obtained ACCY% of 81.25, 90.46 SENY%, and 70.82 SPY%. ECG signal is converted to corresponding 2-D format and fed to 2-D CNN and obtained ACCY% of 98.82 [43]. Sharma and Sunkaria [46] employed random forest algorithm (RFAM) for the categorization of Vfib Vta from non-Vfib Vta and obtained ACCY% of 95.66. Phong and Thien [47] succeeded in obtaining ACCY% of 91.3 by employing RFAM while categorizing Vfib. For computerized external defibrillation and patient monitoring, accurate detection and classification of Vfib, Vfl, and Vta is critical. As a result, having a precise technique to discriminate between Vfib, Vfl, and Vta is critical. Mjahad *et al.* [41] used ANN is employed for classification of Vfib in 2-D (time-frequency representation) and achieved an ACCY% of 98.19, SEN% of 95.56, and SPY% of 98.8. They employed a bagging classifier for the classification of Vfib in 2-D and were able to achieve 98.44 ACCY%, 98.46 SEN%, and 98.43 SPY%. Our proposed technique has achieved significantly better performance when compared with others in terms of ACCY% and SPY%. The proposed parameter set in [44], is a trustworthy technique for automatic external defibrillator shock advisory techniques because it combines reliable detection and prediction, along with the notion that the decision for defibrillation will take into account both the kind of rhythm and the likelihood of successful defibrillation. The technique used in [49] achieved better SPY% when compared with others. With the help

of empirical mode decomposition (EMD) as well as approximate entropy, [48] developed a new technique for detecting Vfib that successfully achieved an ACCY% of 91. It is therefore obvious that using time-frequency information results in higher performance. Last but not least, the success of the proposed method demonstrates that any accuracy loss resulting from feature selection may be avoided by feeding the neural network directly with the time-frequency representation, enabling the creation of higher-performing arrhythmia detectors.

5.   CONCLUSION

The ECG signal is filtered using a two-stage median filter in the proposed approach for the identification of ventricular arrhythmias, followed by a four-stage cascaded SG filter. The outcome of preprocessing stage is then segmented and normalised. Additionally, the 1-D ECG signal is converted into a time-frequency (2-D) representation and provided as an input to a Bi-LSTM network. Eight different classification scenarios are used while classifying things. We have achieved 99.67% and 99.87% average accuracy for 1-D ECG and its 2-D representation, respectively. The suggested approach can be used for automated classification of Ventricular arrhythmias. The performance of the suggested technique can be improved by finely tuning the network parameters. The proposed method can be extended to categorization of other cardiovascular disorders. Hence, the load on the health care professionals can be minimized.

DATA AVAILABILITY STATEMENT

The supporting data for these findings is accessible to the public at the following URL: https://archive.physionet.org/cgi-bin/atm/ATM.

REFERENCES

[1]   R. M. Rangayyan, *Biomedical signal analysis*. John Wiley & Sons 2019.
[2]   World Health Organization, *World health statistics 2015*, WHO. [Online]. Available: https://www.who.int/docs/default-source/gho-documents/world-health-statistic-reports/world-health-statistics-2015.pdf.
[3]   B. H. Rao *et al.*, "Contribution of sudden cardiac death to total mortality in India — A population based study," *International Journal of Cardiology*, vol. 154, no. 2, pp. 163-167, 2012, doi: 10.1016/j.ijcard.2010.09.016.
[4]   A. Ibaida and I. Khalil, "Distinguishing between ventricular Tachycardia and Ventricular Fibrillation from compressed ECG signal in wireless Body Sensor Networks," *2010 Annual International Conference of the IEEE Engineering in Medicine and Biology*, 2010, pp. 2013-2016, doi: 10.1109/IEMBS.2010.5627888.
[5]   H. -B. Xie, G. Z. -Mei, and H. Liu, "Classification of ventricular tachycardia and fibrillation using fuzzy similarity-based approximate entropy," *Expert Systems with Applications*, vol. 38, no. 4, pp. 3973-3981, 2011, doi: 10.1016/j.eswa.2010.09.058.
[6]   J. A. Gomes, *Heart Rhythm Disorders: History, Mechanisms, and Management Perspectives*, Springer Nature, 2020.
[7]   J. Rahul and L. D. Sharma, "Artificial intelligence-based approach for atrial fibrillation detection using normalised and short-duration time-frequency ECG," *Biomedical Signal Processing and Control*, vol. 71, 2022, doi: 10.1016/j.bspc.2021.103270.
[8]   A. Ebrahimzadeh and A. Khazaee, "Detection of premature ventricular contractions using MLP neural networks: A comparative study," *Measurement*, vol. 43, no. 1, pp. 103-112, 2010, doi: 10.1016/j.measurement.2009.07.002.
[9]   E. D. Übeyli, "Statistics over features of ECG signals," *Expert Systems with Applications*, vol. 36, no. 5, pp. 8758–8767, 2009, doi: 10.1016/j.eswa.2008.11.015.
[10]   Y. Toulni, N. Benayad, and B. D. Taoufiq, "Electrocardiogram signals classification using discrete wavelet transform and support vector machine classifier," *IAES International Journal of Artificial Intelligence (IJ-AI)*, vol. 10, no. 4, pp. 960-970, 2021, doi: 10.11591/ijai.v10.i4.pp960-970.
[11]   H. Castro, J. D. G. -Racines, and A. B. -Noreña, "Methodology for detection of paroxysmal atrial fibrillation based on p-wave, hrv and qr electrical alternans features," *International Journal of Electrical and Computer Engineering*, vol. 10, no. 4, 2020, pp. 4023–4034, doi: 10.11591/ijece.v10i4.pp4023-4034.
[12]   K. S. Nugroho, A. Y. Sukmadewa, A. Vidianto, and W. F. Mahmudy, "Effective predictive modelling for coronary artery diseases using support vector machine," *Effective predictive modelling for coronary artery diseases using support vector machine*, vol. 11, no. 1, pp. 345–355, 2022, doi: 10.11591/ijai.v11.i1.pp345-355.
[13]   O. Asmae, R. Abdelhadi, C. Bouchaib, and S. Sara, "Parkinson's diagnosis hybrid system based on deep learning classification with imbalanced dataset," *International Journal of Electrical and Computer Engi-neering (IJECE)*, vol. 13, no. 3, pp. 3204-3216, 2023, doi: 10.11591/ijece.v13i3.pp3204-3216.
[14]   S. Gebeyehu, W. Wolde, and Z. Shibeshi, "Information extraction model from Ge'ez texts," *Indonesian Journal of Electrical Engineering and Computer Science*, vol. 30, no. 2, pp. 787–795, 2023, doi: 10.11591/ijeecs.v30.i2.pp787-795.
[15]   B. Gowrishankar and N. Bhajantri, "Raga classification using enhanced spatial bound whale optimization algorithm," *Indonesian Journal of Electrical Engineering and Computer Science*, vol. 30, no. 2, pp. 825-837, 2023, doi: 10.11591/ijeecs.v30.i2.pp825-837.
[16]   S. Sanmugam, A. Geetha, and L. Parthiban, "Study and innovation of effective classification of XML documents using an advanced deep learning approach," *Indonesian Journal of Electrical Engineering and Computer Science*, vol. 29, no. 3, pp. 1551–1559, 2023, doi: 10.11591/ijeecs.v29.i3.pp1551-1559.
[17]   Ferdiansyah, S. H. Othman, R. Z. Md Radzi, D. Stiawan, and T. Sutikno, "Hybrid gated recurrent unit bidirectional-long short-term

memory model to improve cryptocurrency prediction accuracy," *IAES International Journal of Artificial Intelligence (IJ-AI)*, vol. 12, no. 1, pp. 251–261, 2023, doi: 10.11591/ijai.v12.i1.pp251-261.

[18] S. Hansun, F. P. Putri, A. Q. M. Khalik, H. Hugeng, "On searching the best mode for forex forecasting: bidirectional long short-term memory default mode is not enough," *IAES International Journal of Artificial Intelligence (IJ-AI)*, vol. 11, no. 4, pp. 1596–1606, 2019, doi: 10.11591/ijai.v11.i4.pp1596-1606.

[19] T. Mathu and K. Raimond, "A novel deep learning architecture for drug named entity recognition," *TELKOMNIKA (Telecommunication Computing Electronics and Control)*, vol. 19, no. 6, pp. 1884-1891, 2021, doi: 10.12928/telkomnika.v19i6.21667.

[20] Y. Xia, N. Wulan, K. Wang, and H. Zhang, "Detecting atrial fibrillation by deep convolutional neural networks," *IEEE Access*, vol. 93, pp. 84–92, 2018, doi:10.1016/j.compbiomed.2017.12.007.

[21] S. Stanković, "Time-Frequency Analysis and Its Application in Digital Watermarking," *EURASIP Journal on Advances in Signal Processing*, pp. 1–20, 2010, doi: 10.1155/2010/579295.

[22] R. G. Baraniuk and D. L. Jones, "A signal-dependent time-frequency representation: optimal kernel design," *EEE Transactions on Signal Processing*, vol. 41, no. 4, pp. 1589-1602, 1993, doi: 10.1109/78.212733.

[23] F. Hlawatsch and R. L. Urbanke, "Bilinear time-frequency representations of signals: the shift-scale invariant class," *IEEE Transactions on Signal Processing*, vol. 42, no. 2, pp. 357-366, 1994, doi: 10.1109/78.275608.

[24] M. G. Amin and W. J. Williams, "High spectral resolution time-frequency distribution kernels," *IEEE Transactions on Signal Processing*, vol. 46, no. 10, pp. 2796-2804, 1998, doi: 10.1109/78.720381.

[25] A. L. Goldberger *et al.*, "PhysioBank, PhysioToolkit, and PhysioNet: Components of a new research resource for complex physiologic signals," *Circulation*, vol. 101, no. 23, 2000, doi: 10.1161/01.CIR.101.23.e215.

[26] F. Nolle, F. Badura, J. Catlett, R. Bowser, and M. Sketch, "Crei-gard, a new concept in computerized arrhythmia monitoring systems," *Computers in Cardiology*, pp. 515–518, 1987.

[27] L. D. Sharma and R. K. Sunkaria, "Inferior myocardial infarction detection using stationary wavelet transform and machine learning approach," *Signal, Image and Video Processing*, vol. 12, pp. 199-206, 2018, doi: 10.1007/s11760-017-1146-z.

[28] M. K. Chaitanya and L. D. Sharma, "Electrocardiogram signal filtering using circulant singular spectrum analysis and cascaded Savitzky-Golay filter," *Biomedical Signal Processing and Control*, vol. 75, 2022, doi: 10.10.1016/j.bspc.2022.103583.

[29] K. Feng and Z. Fan, "A novel bidirectional LSTM network based on scale factor for atrial fibrillation signals classification," *Biomedical Signal Processing and Control*, vol. 76, 2022, doi: 10.1016/j.bspc.2022.103663.

[30] R. Panda, S. Jain, R. Tripathy, and U. R. Acharya, "Detection of shockable ventricular cardiac arrhythmias from ECG signals using FFREWT filter-bank and deep convolutional neural network," *Computers in Biology and Medicine*, vol. 124, 2020, doi: 10.1016/j.compbiomed.2020.103939.

[31] N. Sairamya, L. Susmitha, S. T. George, and M. Subathra, "Hybrid Approach for Classification of Electroencephalographic Signals Using Time–Frequency Images With Wavelets and Texture Features," *Intelligent Data Analysis for Biomedical Applications*, pp. 253-273, 2019, doi: 10.1016/B978-0-12-815553-0.00013-6.

[32] B. Boashash, "Estimating and interpreting the instantaneous frequency of a signal. I. Fundamentals," *Proceedings of the IEEE*, vol. 80, no. 4, pp. 520-538, 1992, doi: 10.1109/5.135376.

[33] A. Vakkuri *et al.*, "Time-frequency balanced spectral entropy as a measure of anesthetic drug effect in central nervous system during sevoflurane, propofol, and thiopental anesthesia," *Acta Anaesthesiologica Scandinavica*, vol. 48, no. 2, pp. 145–153, 2004, doi:10.1111/j.0001-5172.2004.00323.x.

[34] S. Hochreiter and J. Schmidhuber, "Long short-term memory," *Neural computation*, vol. 9, no. 8, 1735–1780, 1997, doi: 10.1162/neco.1997.9.8.1735.

[35] A. Sherstinsky, "Fundamentals of Recurrent Neural Network (RNN) and Long Short-Term Memory (LSTM) network," *Physica D: Nonlinear Phenomena*, vol. 404, 2020, doi: 10.1016/j.physd.2019.132306.

[36] Ö. Yildirim, "A novel wavelet sequence based on deep bidirectional LSTM network model for ECG signal classification," *Computers in Biology and Medicine*, vol. 94, pp. 189-202, 2018, doi: 10.1016/j.compbiomed.2018.03.016.

[37] A. Graves, S. Fernández, and J. Schmidhuber, "Bidirectional LSTM Networks for Improved Phoneme Classification and Recognition," *Artificial Neural Networks: Formal Models and Their Applications – ICANN 2005*, 2005, vol. 3697, doi: 10.1007/11550907_126.

[38] M. Schuster and K. K. Paliwal, "Bidirectional recurrent neural networks," *IEEE Transactions on Signal Processing*, vol. 45, no. 11, pp. 2673-2681, 1997, doi: 10.1109/78.650093.

[39] E. J. da S. Luz, W. R. Schwartz, G. C. -Chávez, and D. Menotti, "ECG-based heartbeat classification for arrhythmia detection: A survey," *Computer Methods and Programs in Biomedicine*, vol. 127, pp. 144-164, 2016, doi: 10.1016/j.cmpb.2015.12.008.

[40] S. Gudmundsson, T. P. Runarsson, and S. Sigurdsson, "Test–retest reliability and feature selection in physiological time series classification," *Computer Methods and Programs in Biomedicine*, vol. 105, no. 1, pp. 50-60, 2012, doi: 10.1016/j.cmpb.2010.08.005.

[41] A. Mjahad, A. R, -Muñoz, M. B. -Mompeán, J. V. F. -Víllora, and J. F. G. -Martínez, "Ventricular Fibrillation and Tachycardia detection from surface ECG using time-frequency representation images as input dataset for machine learning," *Computer Methods and Programs in Biomedicine*, vol. 141, pp. 119-127, 2017, doi: 10.1016/j.cmpb.2017.02.010.

[42] D. Panigrahy, P. Sahu, and F. Albu, "Detection of ventricular fibrillation rhythm by using boosted support vector machine with an optimal variable combination," *Computers and Electrical Engineering*, vol. 91, 2021, doi: 10.1016/j.compeleceng.2021.107035.

[43] S. Mandal, P. Mondal, and A. H. Roy, "Detection of Ventricular Arrhythmia by using Heart rate variability signal and ECG beat image," *Biomedical Signal Processing and Control*, vol. 68, 2021, doi: 10.1016/j.bspc.2021.102692.

[44] I. Jekova, "Shock advisory tool: Detection of life-threatening cardiac arrhythmias and shock success prediction by means of a common parameter set," *Biomedical Signal Processing and Control*, vol. 2, no. 1, 2007, doi: 10.1016/j.bspc.2007.01.002.

[45] Q. Li, C. Rajagopalan and G. D. Clifford, "Ventricular Fibrillation and Tachycardia Classification Using a Machine Learning Approach," *IEEE Transactions on Biomedical Engineering*, vol. 61, no. 6, pp. 1607-1613, 2014, doi: 10.1109/TBME.2013.2275000.

[46] L. D. Sharma and R. K. Sunkaria, "Stationary wavelet transform based technique for automated external defibrillator using optimally selected classifiers," *Measurement*, vol. 125, pp. 29-36, 2018, doi: 10.1016/j.measurement.2018.04.054.

[47] P. A. Phong and K. Q. Thien, "Classification of Cardiac Arrhythmias Using Interval Type-2 TSK Fuzzy System," *2009 International Conference on Knowledge and Systems Engineering*, 2009, pp. 1-6, doi: 10.1109/KSE.2009.19.

[48] L. Kaur and V. Singh, "Ventricular Fibrillation Detection using Empirical Mode Decomposition and Approximate Entropy," *International journal of emerging technology and advanced engineering*, vol. 3, no. 5, pp. 260–268, 2013.

[49] H. Fujita and D. Cimr, "Computer Aided detection for fibrillations and flutters using deep convolutional neural network," *Information Sciences*, vol. 486, pp. 231–239, 2019, doi: 10.1016/j.ins.2019.02.065.

BIOGRAPHIES OF AUTHORS

M Krishna Chaitanya is currently pursuing Ph.D. in School of Electronic Engineering at VIT-AP University. He received M.Tech. in the year 2008 from Kakatiya Institute of Technology and Science, Wagarangal, Telangana, India. His research areas include biomedical signal processing, deep learning, machine learning, and ECG signal filtering. He can be contacted at email: kchaitanya277@gmail.com.

Lakhan Dev Sharma received the Ph.D. degree from Dr B. R. Ambedkar National Institute of Technology Jalandhar, India, in 2018 and M.Tech. degree from Atal Bihari Vajpayee-Indian Institute of Information Technology and Management, Gwalior, India, in 2012. He has been serving as a Associate Professor with the School of Electronics Engineering, VIT-AP University, Amaravati, India since 2020. He has teaching experience at various technical institutes and university levels. His research interests include biomedical signal and image processing, machine learning, and deep learning. He is an editorial board member of frontiers in Signal Processing (Biomedical Signal Processing) and frontiers in Physiology (Computational Physiology and Medicine) Journal. He can be contacted at email: devsharmalakhan@gmail.com.